JOURNAL OF AGRICULTURAL AND FOOD CHEMISTRY

Article

Cite This: J. Agric. Food Chem. 2018, 66, 6889−6896

pubs.acs.org/JAFC

Fabrication of a Flexible Gold Nanorod Polymer Metafilm via a Phase Transfer Method as a SERS Substrate for Detecting Food Contaminants

Nan Yang, Ting-Ting You,* Yu-Kun Gao, Chen-Meng Zhang, and Peng-Gang Yin*

Key Laboratory of Bio-Inspired Smart Interfacial Science and Technology of Ministry of Education, School of Chemistry, Beihang University, Beijing 100191, China

Supporting Information

ABSTRACT: Surface enhanced Raman scattering (SERS) has been widely used in detection of food safety due to the nondestructive examination property. Here, we reported a flexible SERS film based on a polymer-immobilized gold nanorod polymer metafilm. Polystyrene−polyisoprene−polystyrene (SIS), a transparent and flexible, along with having excellent elasticity, polymer, was chosen as the main support of gold nanorods. A simple phase transfer progress was adopted to mix the gold nanorods with the polymer, which can further be used in most water-insoluble polymers. The SERS film performed satisfactorily while being tested in a series of standard Raman probes, like crystal violet (CV) and malachite green (MG). Moreover, the excellent reproducibility and elastic properties make the film a promising substrate in practical detection. Hence, the MG detection on the fish surface and trace thiram detection on orange pericarp were inspected with detection results of 1×10^{-10} and 1×10^{-6} M, which were below the demand of the National standard of China, exactly matching the realistic application requirements.

KEYWORDS: *surface-enhanced Raman scattering, phase transfer, gold nanorods, flexible film, food safety*

INTRODUCTION

Surface enhanced Raman scattering (SERS) has been considered a powerful tool in analytical chemistry, biological detection, food safety, and environment monitoring with unique advantages of nondestructive examination.[1−7] In recent decades, many efforts have been made to develop the novel strategy of fabricating SERS-active substrates for the sensitive analysis of food contaminants.[8−11] Due to the localized surface plasmon resonance (LSPR) effect, noble metal nanomaterials could be applied as building blocks to fabricate a SERS substrate with enhanced electromagnetic field intensities.[12] The metallic nanoparticle suspensions were widely chosen as a media of a SERS substrate; however, the aggregation and coagulation are major limitations.[13] An improved substrate that immobilized the nanoparticles on solid materials enhanced the reproducibility and homogeneity, but a main drawback exists that it cannot make contact with the detection object that is conformally caused by the rigid support.[14] Hence, flexible SERS substrates are desperately desired for practical application on nonplanar objects. Up to now, different materials were adopted as flexible SERS substrates, such as metal foil, paper-based materials, and polymers.[15−19] Among those materials, polymers show a high transparency and great elastic deformation which are fit for collecting Raman signals from both sides.[20] A flexible polymer−metal SERS substrate has always been used on irregular surfaces as a pesticide detection for fruits pericarp, bacteria collection, and recognition on a spinach leaf.[17,21−28]

Fabricating a flexible polymer metafilm SERS substrate with great SERS intensity and reproductivity using a simpe approach is useful for realistic application. Traditional fabrication approaches for a flexible metal−polymer substrate include deposition, electrospinning, and imprinting lithograph.[29−34] However, certain drawbacks exist, such as high cost, time-consuming, and the conditions are only allowed in the laboratory. So, an effective flexible metal−polymer SERS substrate with a cheap price and simple fabrication method is desired. Bell's group proposed poly-SERS films formed by simply mixing prepared Au/Ag nanoparticle aggregating colloids with polymer powder, which were then dried as a film suitable for a portable Raman spectrometer.[35,36] This method is easily inspired as a mixture polymer and noble nanoparticle. For most water-insoluble polymers, transferring metal nanoparticles from the common water phase to their organic solvent will broaden the types and applications of these metafilms.

Herein, we report a polystyrene−polyisoprene−polystyrene (SIS)-immobilized gold nanorod cluster metafilm as a SERS substrate via a simple and convenient method. The SIS, a commercially flexible polymer, acted as not only a flexible, transparent, and Raman noiseless base but also a stretch support of gold nanorods, which ensured the sensitivity and reproducibility along with the good elastic property of this metafilm. A phase transfer process was first adopted to mix the dichloromethane (DCM) resolvent gold nanorods with SIS, then the resolvent was evaporated, and the thin film was obtained. Using CV (crystal violet) and MG (malachite green)

Received: April 2, 2018
Revised: May 12, 2018
Accepted: June 8, 2018
Published: June 8, 2018

DOI: 10.1021/acs.jafc.8b01702
J. Agric. Food Chem. 2018, 66, 6889−6896

Scheme 1. Phase Transfer and Film Fabrication Progress

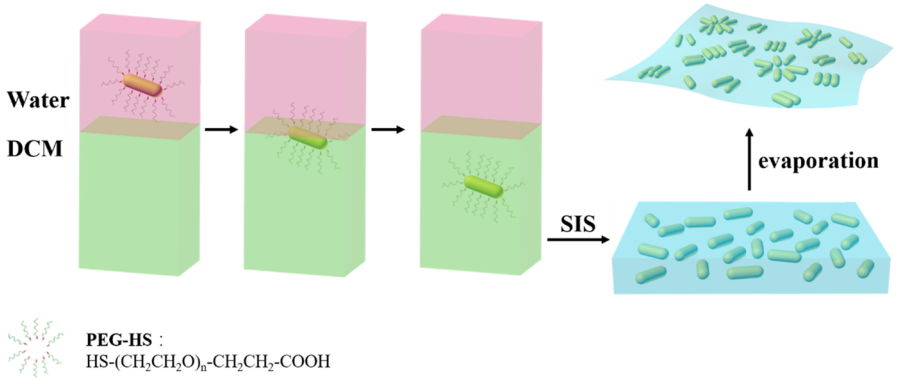

as SERS probes, the detection concentrations are as low as 1×10^{-9} and 1×10^{-10} M, and the enhancement factors (EF) were calculated as 4.5×10^6 and 4×10^6. Practical examination of MG detection on the fish surface and thiram detection on orange pericarp were carried out with a detection concentration of 1×10^{-10} and 1×10^{-6} M (0.2 ppm), which is far below the National standard of China (GB) of 1×10^{-9} and 1×10^{-5} M (5 ppm). The excellent SERS performance implies a broad application on food safety and detection of pesticide residue detection.

MATERIALS AND METHODS

Reagents. Chloroauric acid ($HAuCl_4$) and polystyrene-*block*-polyisoprene-*block*-polystyrene (SIS, styrene 17 wt %) were purchased from Sigma-Aldrich (Shanghai, China). Thiolated polyethylene glycol (PEG-SH, MW 5000 Da) was purchased from Aladdin (Shanghai, China). Cetyltrimethyl ammonium bromide (CTAB) was purchased from Lanyi Factory Co. (Beijing, China). Sodium oleate (NaOL) was purchased from Hushi Laboratory Equipment Co. (Shanghai, China). Silver nitrate ($AgNO_3$) and sodium borohydride ($NaBH_4$) were purchased from Guanghua Chemical Factory Co. (Guangdong, China). Ascorbic acid (AA) was purchased from Xilong Factory Co. (Guangdong, China). All of the syntheses processes used Ultrapure Milli-Q water. All of the glassware was cleaned with aqua regia, rinsed with Milli-Q water multiple times, and then dried before use.

Synthesis of the Gold Nanorods (AuNRs). Monodisperse AuNRs were synthesized using a seed-mediated growth method.[37] First, 5 mL of $HAuCl_4$ solution (0.5 mM) with 5 mL of CTAB (0.2M) solution were mixed, followed by the addition of 0.6 mL of fresh ice $NaBH_4$ (0.01M), which was diluted with 1 mL of pure water. The mixture was kept under vigorous stirring for 2 min and incubated as a seed solution for at least 30 min before being used at room temperature. Next, 3.5 g of CTAB and 0.617 g of NaOL were dissolved in a 250 mL flask, and then 9 mL of AgNO3 solution (4 mM) was added. The solution was undisturbed for 15 min at 30 °C, and then 125 mL of $HAuCl_4$ solution (1 mM) was added. The mixture was stirred at 700 rpm for 90 min followed by the addition 0.75 mL of HCl to adjust the PH, and then the mixture was slowly stirred for 15 min at 400 rpm. Finally, 0.625 mL of ascorbic acid (0.064 M) and 0.2 mL of gold seed solution were added, and the mixture stirred at 1200 rpm for 30 s after each step. The solution was kept undisturbed at 30 °C for 12 h and then was centrifuged at 7000 rpm for 20 min three times to obtain the final products, an isochoric solution of AuNRs and 10 mL of ultrapure water.

Fabrication of Gold Nanorod/PMMA Flexible Substrates. To form the thin flexible film, a phase transfer progress was adopted, and thiolated polyethylene glycol (PEG-SH) was used as a phase transfer agent, which was used to commonly modify nanoparticles, particularly those that can be dissolved both in water and DCM (the solvent of SIS).[38,39] First, 1 mL of the previously prepared AuNRs solution was diluted to 2 mL, and then it was added to 2 mL of PEG-SH DCM solution (0.1%). There was an obvious two-phase interface that existed with the organic phase beneath the water phase. Next, following the addition of 3 mL of methanol to dilute the AuNRs solution, the solution was shaken, and an emulsion formed and displayed a milk pink color. Then, another 2 mL of methanol was added, and the mixture was shaken until it formed a monophasic system. Finally, after 1 mL of water was added, the PEG-SH-capped AuNRs were transferred from the upper layer to the lower layer, which indicated the transfer from the water phase to the DCM phase. The AuNRs were washed using an isochoric process with 2 mL of DCM three times.

Next, 20 mg of SIS was added to different volumes of the AuNR–DCM solution (from 200 to 600 μL), and the mixture was stirred until the polymer completely dissolved, approximately 5–10 min. Finally, the polymer–AuNR solution was poured into a polytetrafluoroethylene mold (diameter 2 cm, height 0.5 cm), DCM solvent was evaporated at room temperature for about 30 min, and then the thin flexible polymer metalfilm was obtained.

Fabrication of SERS Sample. For the SERS sensitivity measurement, pieces of the polymer metalfilm were soaked in a series of standard CV (from 10^{-5} to 10^{-9} M) and MG (from 10^{-6} to 10^{-10} M) solution for 4 h. For MG detection on the fish surface, the fish was immersed in MG solution with different concentrations (10^{-8}–10^{-10} M) for 15 min, then it was taken out, and thepolymer metalfilm was directly covered. For thiram detection on the orange pericarp, 10^{-6} M thiram was sprayed onto small pieces of orange pericarp, and then the polymer metalfilm was covered.

Characterization. Field emission scanning electron microscopy (FE-SEM) was performed on a Jeol-JSM 7500 scanning electron microscope (SEM) with an accelerating voltage of 5.0 kV. The UV–vis spectrophotometer and fittings were provided by Shimadzu (Japan) Co., Ltd. Raman spectra were recorded with a JY HR800 Raman spectrometer (HORIBA Jobin Yvon), equipped with a 50× objective (NA = 0.5) and a He–Ne laser with a 633 nm wavelength; the laser power values measured in the experiments were obtained from a power meter (0.75 mW at the samples with a spot area of approximately 1.4 μm^2). The Raman band of a silicon wafer at 520.8 cm^{-1} was used to calibrate the spectrometer. Chromatographic analysis was performed with an HPLC instrument (Shimadzu, LC-20A, Japan), which consisted of a water pump, a reverse-phase C-18 column (Inertsil ODS-SP, 4.6 mm × 150 mm, particle size 5 μm), an ultraviolet detector, and a 20-μL injection loop. The mobile phase was a mixture of acetonitrile (ACN) and 50 mmol L^{-1} pH 4.5 acetate buffer (4:1, v/v), and its flow rate was 0.4 mL min^{-1}. The detection wavelength was set to 300 nm.

RESULTS AND DISCUSSION

Mechanism Analysis. The phase transfer and film fabrication progress are illustrated in Scheme 1. The PEG-SH can dissolve both in the water and DCM phase due to the hydrophilic and hydrophobic groups. The sulfhydryl group can

DOI: 10.1021/acs.jafc.8b01702
J. Agric. Food Chem. 2018, 66, 6889–6896

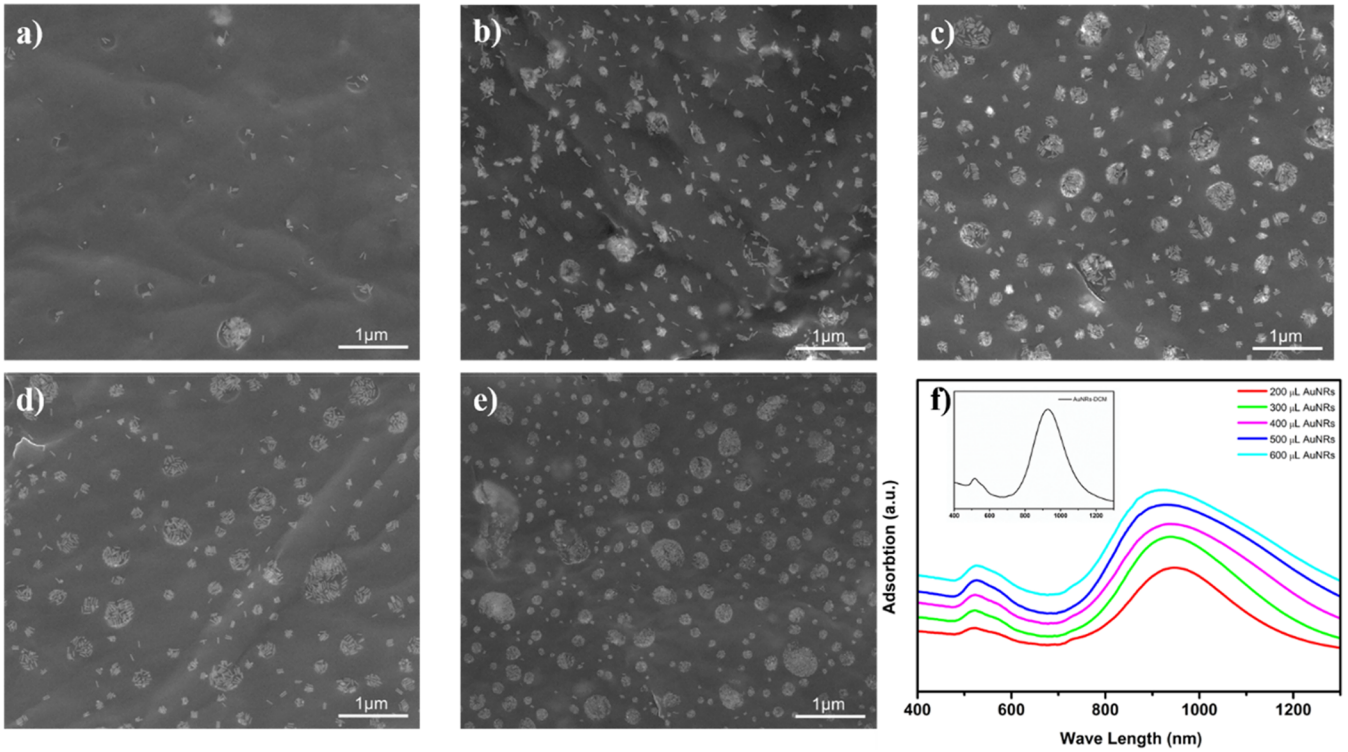

Figure 1. SEM image of metafilm fabrication with different AuNR−DCM solution volumes: (a) 200, (b) 300, (c) 400, (d) 500, and (e) 600 μL. (f) UV−vis spectra of metafilm fabrication with different volume AuNRs, the inset graph shows UV−vis spectra of monodispersed AuNRs in DCM solution.

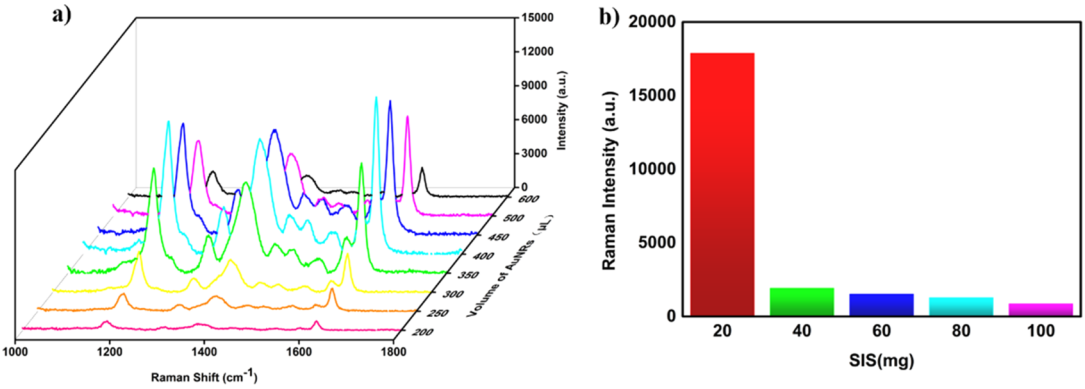

Figure 2. (a) SERS spectra of metafilm fabrication with different volumes of AuNR−DCM solution: red line, 200; orange line, 250; yellow line, 300; green line, 350; cyan line, 400; blue line, 450; pink line, 500; and black line, 600 μL. The laser wavelength is 633 nm, and the integration time is 1 s. (b) SERS intensity at 1620 cm^{-1} of CV on substrates prepared with different amounts of SIS.

capture AuNRs through the Au−S bond in those two phases, which help transfer AuNRs from the water phase to the DCM phase. The large molecule weights (MW of 5000 Da) make sure that the phases transfer properly without nanoparticle aggregation.[38,39] After this critical step, we can simply add polymer SIS to the AuNR−DCM solution followed by a stirring approach aimed to dissolve the SIS, and this made the AuNRs monodisperse in this polymer organic solution. Finally, an evaporation progress was adopted to obtain the thin metafilm.

Optical Characterization. The SEM images of different quantities of AuNRs added into a metafilm are shown in Figure 1a−e, and the TEM image of monodispersed AuNR is shown in Figure S1, in which the nanorods have a ratio of 3.8 (105.34 ± 5.16/27.52 ± 1.44). The monodispersed AuNRs appear side by side as dimer and trimer structures during the formation process of film. As the volume of the AuNR solution increased from 200 to 400 μL, the cluster structures began to occur. By continuing to increase the AuNRs solution volume to 500 μL, the clusters became bigger, and they continued to increase both in size and quantity when the volume reached 600 μL. A proper distance between the coupling nanoparticles is critical to the enhancement of the SERS signal under the "hot spot" effect.[40] The gaps between AuNGs are marked in Figure S2. Figure 1f shows the UV−vis spectra of the metafilm with different quantities of AuNRs added, in which the peaks of monodispersed AuNRs dissolved in DCM appear at 515 and 929 nm, corresponding to the transverse and longitudinal bands of the AuNRs. In the film, as the amount of AuNRs increased, the transverse plasmon band slightly red shifted

DOI: 10.1021/acs.jafc.8b01702
J. Agric. Food Chem. 2018, 66, 6889−6896

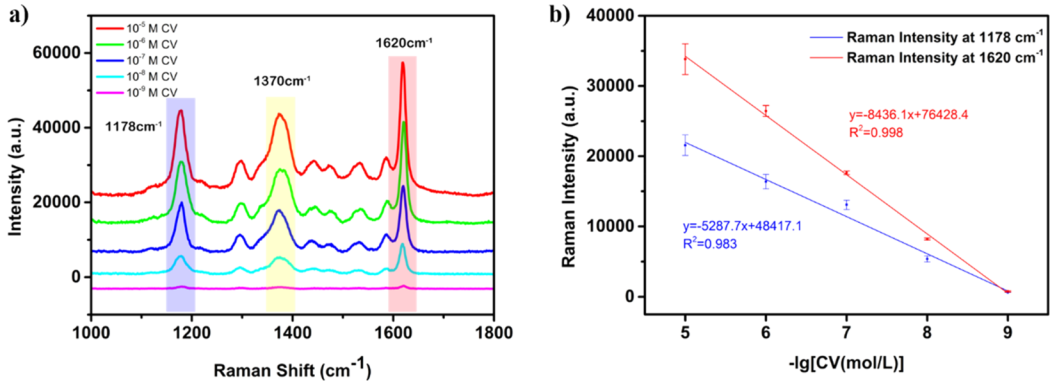

Figure 3. (a) SERS spectra of the metafilm adsorbing different concentrations of CV standard samples from 10^{-5} to 10^{-9} M (red line, 10^{-5}; green line, 10^{-6}; blue line, 10^{-7}; cyan line, 10^{-8}; and pink line, 10^{-9} M). (b) The normalized Raman intensity at 1178 and 1620 cm^{-1} versus the negative logarithms of the thiram concentrations ranging from 10^{-5} to 10^{-9} M.

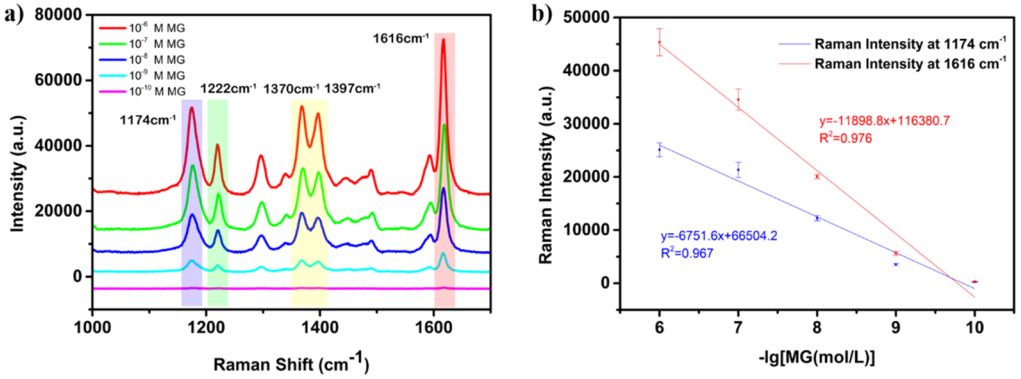

Figure 4. (a) SERS spectra of the metafilm adsorbing different concentrations of MG standard samples from 10^{-6} to 10^{-10} M (red line, 10^{-6}; green line, 10^{-7}; blue line, 10^{-8}; cyan line, 10^{-9}; pink line, 10^{-10} M). (b) The normalized Raman intensity at 1174 and 1616 cm^{-1} versus the negative logarithms of the thiram concentrations ranging from 10^{-5} to 10^{-9} M.

from 523 to 526 nm, and the longitudinal plasmon band blue shifted from 945 to 915 nm. This result is mainly attributable to the coupling of the plasmons of the side-by-side interacting nanorods.[41] The shift of the plasmon band agreed with the morphology shown in the SEM images.

SERS Performance. The fabricated metafilms were employed in the SERS measurement and the Raman spectra, as shown in Figure 2a. Using CV as the SERS probe, while 400 μL of AuNRs were added, the substrate presents the best SERS performance. When the AuNRs quantities were less than 400 μL, the SERS intensity was higher due to the increased amount of AuNRs. However, continuing to increase the AuNRs quantity will cause excessive aggregates and reduce the SERS intensity, which was verified by the morphology shown in Figure 1. Hence, 400 μL of AuNRs added to the sample was considered as the suitable amount in the next process. The dosage of SIS was also optimized, as shown in Figure 2, and the best result was obtained with 20 mg. The film is hardly formed intact if the amount of polymer SIS is less than 20 mg, to the contrary, adding more than 20 mg will tend to sharply reduce the Raman intensity by completely covering the AuNRs inside the polymer component.

The optimized metafilm was immersed in series of standard CV (from 10^{-5} to 10^{-9} M) solution and then subjected to direct SERS measurements. Four major characteristic peaks could be observed in Figure 3a at 1178, 1296, 1374, and 1620 cm^{-1}, corresponding to in-plane aromatic C−H vibration, C−C ring stretching, in-plane N-phenyl stretching vibration, and in-plane C−C stretching vibration of the ring.[42,43] The lowest detection concentration was 10^{-9} M, and the satisfactory linearity at peaks of 1178 and 1620 cm^{-1} between 10^{-5} and 10^{-9} M were obtained with a correlation coefficient of 0.983 and 0.998, as shown in Figure 3b. The high SERS sensitivity and linearity imply that this flexible SERS substrate could reach application requirements in realistic detection.

The Raman EF was calculated to evaluate the SERS activity of the polymer metafilm by this formula:

$$EF = \frac{I_{SERS}}{I_{NRS}} \times \frac{N_{NRS}}{N_{SERS}}$$

where I_{SERS} and N_{SERS} are normalized Raman peak intensities and the number of the reporter molecule chemisorbed on the SERS substrate; I_{NRS} and N_{NRS} are the same parameters that are in the reference solution.[17,44,45] The CV concentration is 10^{-9} M on the SERS substrate and 10^{-4} M in the reference solution. By substituting the measured and calculated values into the equation, the EF was calculated to be 4.64×10^5, according to the peaks at 1620 cm^{-1} (corresponding SERS spectra are provided in Figure S3).

Furthermore, MG as a parasiticide has been widely used in aquaculture, which may cause water toxicity residue, environmental pollution, and even cancerogenic and genetic aberrant, which has been forbidden for a long time.[46] However, it still illegal to be used due to the low cost and effective antibacterial activity that brought food insecurity and water pollution.[47] In view of the above information, the successful detection of MG

DOI: 10.1021/acs.jafc.8b01702
J. Agric. Food Chem. 2018, 66, 6889−6896

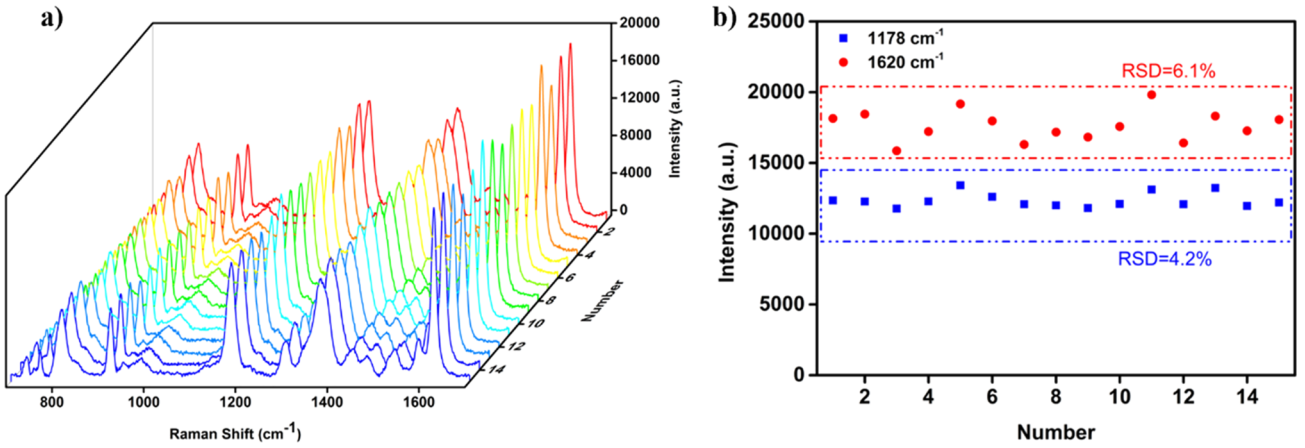

Figure 5. (a) SERS spectra collected from 15 random points on metafilm substrates that have been soaked in 10^{-7} M CV for 4 h. (b) Corresponding RSD results of (a) calculated by SERS intensities for 1178 and 1620 cm^{-1} Raman peaks.

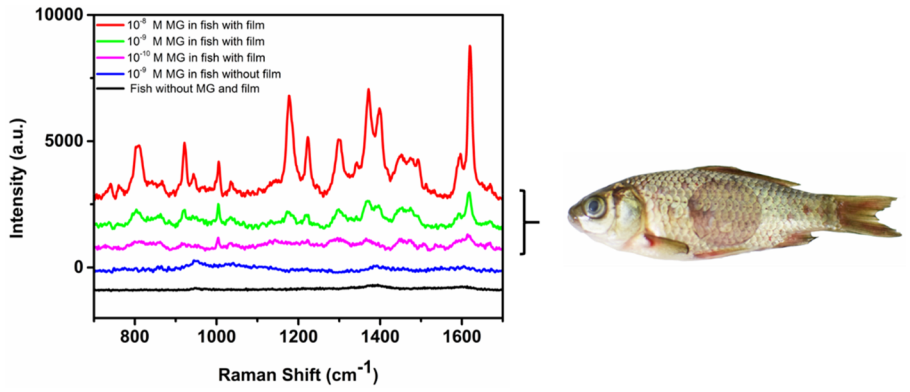

Figure 6. In situ detection of MG on the fish surface under different conditions. The laser wavelength is 633 nm, and the integration time is 15 s.

by our developed SERS substrates gave a promising future to food safety. Figure 4a shows a SERS spectra of an optimized metafilm soaked in different concentrations of standard MG (from 10^{-6} to 10^{-10} M) solution. The peaks at 1174, 1296, 1368, and 1616 cm^{-1} are the same as CV due to the similar structures.[43,47] The peaks at 1220 and 1396 cm^{-1} correspond to the C−H ring in-plane bending vibrations and C−H ring in-plane bending.[42,46−48] Figure 4a indicated that, while the concentration is as low as 10^{-10} M, peaks at 1174 and 1616 cm^{-1} still can be found. The satisfactory linearity at peaks of 1174 and 1616 cm^{-1} between 10^{-6} and 10^{-10} M were obtained with a correlation coefficient of 0.967 and 0.976 in Figure 4b. The EF was calculated to be 4×10^6, according to peaks at 1616 cm^{-1} (corresponding SERS spectra are provided in Figure S3).

SERS Reproducibility. To measure the SERS reproducibility of the flexible substrate, we collected the SERS spectra of 15 random points, which is displayed in Figure 5a, and SERS spectra collected from substrate-to-substrate is provided in Figure S4. The signal intensity distribution at 1178 and 1620 cm^{-1} is shown in Figure 5b with an intensity variation of 4.2% and 6.1%. These results mainly serve as the reasonable reproducibility and imply a good homogeneity of the substrate.

Considering the excellent elastic deformation of the SIS polymer, we also tested the Raman intensity of a flexible metafilm under the different stretching ratio, the result is shown in Figure S5, no obvious change is observed under the stretching status, indicating the promising detection application on the surface of irregular objects. The good SERS performance with high sensitivity and reproducibility of the flexible polymer metafilm ensures that the substrate is satisfying the demands of realistic application.

Practical Application. Several SERS detections were carried out on real-world objects to prove the practicability of the obtained flexible polymer metafilm SERS substrate. The fish was soaked in a MG molecular and then covered with the film directly on it; we were able to collect the SERS signal while the laser irradiated the film. As shown in Figure 6, obvious characteristic peaks could be observed, and the peak at 1616 cm^{-1} still can be distinguished even with a MG concentration as low as 1×10^{-10} M, which is below the national standard of China (GB 19857-2005). On the contrary, there is no obvious signal found in fish surface without the metafilm covering it and using the same MG concentration. The SERS spectrum collected from the fish surface with 10^{-9} M MG at different immersion times is provided in Figure S6. The spectrum collected from the fish surface immersed in 10−9 M MG for 30 min is similar to that of 15 min. Thus, using 15 min-immersed fish was reasonable for practical application. High-performance liquid chromatography (HPLC) was adopted to validate the SERS method, Figure S7 shows 10^{-5} M MG detected by SERS and HPLC. The result indicates the accuracy of SERS detection based on this metafilm, and the high sensitivity makes this film a promising substrate for practical food safety detection. Furthermore, we applied the same method to detect trace pesticide thiram (TMTD,

DOI: 10.1021/acs.jafc.8b01702
J. Agric. Food Chem. 2018, 66, 6889−6896

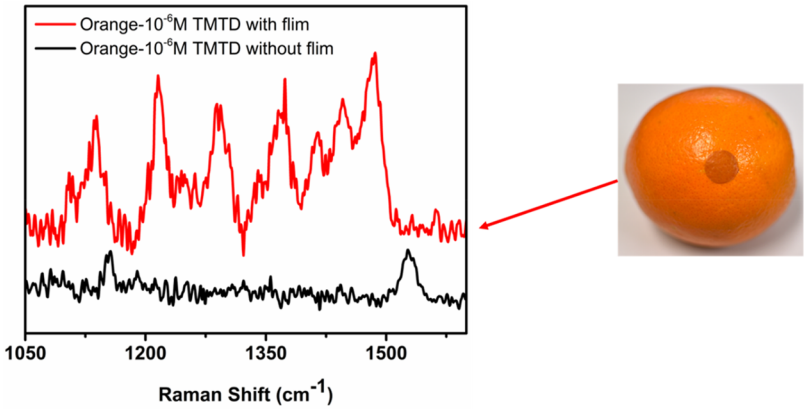

Figure 7. In situ detection of thiram on orange pericarp under different conditions. The laser wavelength is 785 nm, and the integration time is 10 s.

tetramethyl thiuram disulfide) on fruit skin, and it is shown in Figure 7.[49] Major peaks at 1374 cm^{-1} can be obtained simply by covering the film on thiram-immersed orange pericarp with a concentration of 1×10^{-6} M (0.24 ppm), which is lower than 5 ppm according to the national standard of China (GB 2763-2016). Food contaminant residues detected by SERS in related literatures are compared in Table S1. Considering the ease of fabrication, simple signal collection, and excellent SERS performance, this flexible metafilm can serve as a promising platform in the applications of food safety inspection and trace detection of pesticide residuals.

In summary, a simple phase transfer and evaporation progress was first adopted to form the flexible and transparent SERS polymer metafilm. This method can further be used to combine most of the water-insoluble polymers with metal nanoparticles. The optimized SERS film exhibits fantastic flexibility and stability along with an elastic property provided by polymer support, as well as an excellent SERS performance due to the AuNRs. The sensitivity of the SERS substrate was proven by a Raman test on CV and MG with minimum detection concentrations of 1×10^{-9} and 1×10^{-10} M, respectively. The high sensitivity and flexibility with the signal stability during the stretching behavior make the film a promising substrate for practical food safety detection. The detection concentration for MG on the fish surface and thiram on orange pericarp could reach 1×10^{-10} and 1×10^{-6} M, which is much lower than the GB demand. This flexible SERS metafilm is expected to further application in food safety detection.

■ ASSOCIATED CONTENT

Supporting Information

The Supporting Information is available free of charge on the ACS Publications website at DOI: 10.1021/acs.jafc.8b01702.

Results demonstrating the TEM images of AuNRs, the gaps between goldnanorods in 400 μL of AuNR−DCM fabricated metafilm using the high-magnification SEM image, SERS spectra of 10^{-3} M CV and 10^{-3} M MG, SERS spectra collected from five metafilm substrate samples in the same condition, corresponding Raman intensity change of flexible metafilm under different stretching ratio, SERS spectrum collected from the fish surface with 10−9 M MG in different immersion times, spectrum of 10^{-5} M MG detected by SERS and HPLC, and the table of food contaminant residues detected by SERS with different substrates (PDF)

■ AUTHOR INFORMATION

Corresponding Authors

*E-mail: (T.-T.Y.) youtt@buaa.edu.cn.
*E-mail: (P.-G.Y.) pgyin@buaa.edu.cn.

ORCID

Peng-Gang Yin: 0000-0001-6796-5921

Funding

This work was supported by the National Natural Science Foundation of China (51572009).

Notes

The authors declare no competing financial interest.

■ REFERENCES

(1) Nie, S.; Emory, S. R. Probing Single Molecules and Single Nanoparticles by Surface-Enhanced Raman Scattering. *Science* **1997**, *275*, 1102.
(2) Porter, M. D.; Lipert, R. J.; Siperko, L. M.; Wang, G.; Narayanan, R. SERS as a bioassay platform: fundamentals, design, and applications. *Chem. Soc. Rev.* **2008**, *37*, 1001−11.
(3) Stiles, P. L.; Dieringer, J. A.; Shah, N. C.; Van Duyne, R. P. Surface-enhanced Raman spectroscopy. *Annu. Rev. Anal. Chem.* **2008**, *1*, 601.
(4) Alvarez-Puebla, R. A.; Liz-Marzán, L. M. SERS-Based Diagnosis and Biodetection. *Small* **2010**, *6*, 604−10.
(5) Halvorson, R. A.; Vikesland, P. J. Surface-enhanced Raman spectroscopy (SERS) for environmental analyses. *Environ. Sci. Technol.* **2010**, *44*, 7749.
(6) Doering, W. E.; Nie, S. Single-Molecule and Single-Nanoparticle SERS: Examining the Roles of Surface Active Sites and Chemical Enhancement. *J. Phys. Chem. B* **2002**, *106*, 311−317.
(7) Prawer, S.; Nemanich, R. J. Raman Spectroscopy of Diamond and Doped Diamond. *Philos. Trans. R. Soc., A* **2004**, *362*, 2537.
(8) Li, P.; Dong, R. L.; Wu, Y. P.; Liu, H. L.; Kong, L. T.; Yang, L. B. Polystyrene/Ag nanoparticles as dynamic surface-enhanced Raman spectroscopy substrates for sensitive detection of organophosphorus pesticides. *Talanta* **2014**, *127*, 269−275.
(9) Li, P.; Liu, H. L.; Yang, L. B.; Liu, J. H. The time-resolved D-SERS vibrational spectra of pesticide thiram. *Talanta* **2013**, *117*, 39−44.
(10) Liu, H. L.; Yang, Z. L.; Meng, L. Y.; Sun, Y. D.; Wang, J.; Yang, L. B.; Liu, J. H.; Tian, Z. Q. Three-Dimensional and Time-Ordered Surface-Enhanced Raman Scattering Hotspot Matrix. *J. Am. Chem. Soc.* **2014**, *136*, 5332−5341.

DOI: 10.1021/acs.jafc.8b01702
J. Agric. Food Chem. 2018, 66, 6889−6896

(11) Yang, L. B.; Li, P.; Liu, H. L.; Tang, X. H.; Liu, J. H. A dynamic surface enhanced Raman spectroscopy method for ultra-sensitive detection: from the wet state to the dry state. *Chem. Soc. Rev.* **2015**, *44*, 2837−2848.
(12) Stewart, M. E.; Anderton, C. R.; Thompson, L. B.; Maria, J.; Gray, S. K.; Rogers, J. A.; Nuzzo, R. G. Nanostructured plasmonic sensors. *Chem. Rev.* **2008**, *108*, 494−521.
(13) Guerrini, L.; Graham, D. Molecularly-Mediated Assemblies of Plasmonic Nanoparticles for Surface-Enhanced Raman Spectroscopy Applications. *Chem. Soc. Rev.* **2012**, *21*, 7085−7107.
(14) Fan, M.; Andrade, G. F.; Brolo, A. G. A review on the fabrication of substrates for surface enhanced Raman spectroscopy and their applications in analytical chemistry. *Anal. Chim. Acta* **2011**, *693*, 7.
(15) Holthoff, E. L.; StratisCullum, D. N.; Hankus, M. E. A Nanosensor for TNT Detection Based on Molecularly Imprinted Polymers and Surface Enhanced Raman Scattering. *Sensors* **2011**, *11*, 2700.
(16) Ye, W.; Chen, Y.; Zhou, F.; Wang, C.; Li, Y. Fluoride-assisted galvanic replacement synthesis of Ag and Au dendrites on aluminum foil with enhanced SERS and catalytic activities. *J. Mater. Chem.* **2012**, *22*, 18327−18334.
(17) Webb, J.; Aufrecht, J.; Hungerford, C.; Bardhan, R. Ultra-sensitive analyte detection with plasmonic paper dipsticks and swabs integrated with branched nanoantennas. *J. Mater. Chem. C* **2014**, *2*, 10446−10454.
(18) Yu, C. C.; Chou, S. Y.; Tseng, Y. C.; Tseng, S. C.; Yen, Y. T.; Chen, H. L. Single-shot laser treatment provides quasi-three-dimensional paper-based substrates for SERS with attomolar sensitivity. *Nanoscale* **2015**, *7*, 1667−77.
(19) Yilmaz, M.; Erkartal, M.; Ozdemir, M.; Sen, U.; Usta, H.; Demirel, G. Three Dimensional Au-Coated Electrosprayed Nano-structured BODIPY Films on Aluminum Foil as Surface-Enhanced Raman Scattering Platforms and Their Catalytic Applications. *ACS Appl. Mater. Interfaces* **2017**, *9* (21), 18199.
(20) Xu, K.; Wang, Z.; Tan, C. F.; Kang, N.; Chen, L.; Ren, L.; Thian, E. S.; Ho, G. W.; Ji, R.; Hong, M. Uniaxially Stretched Flexible Surface Plasmon Resonance Film for Versatile Surface Enhanced Raman Scattering Diagnostics. *ACS Appl. Mater. Interfaces* **2017**, *9*, 26341.
(21) Shiohara, A.; Langer, J.; Polavarapu, L.; Liz-Marzán, L. M. Solution processed polydimethylsiloxane/gold nanostar flexible substrates for plasmonic sensing. *Nanoscale* **2014**, *6*, 9817.
(22) Zhong, L. B.; Yin, J.; Zheng, Y. M.; Liu, Q.; Cheng, X. X.; Luo, F. H. Self-Assembly of Au Nanoparticles on PMMA Template as Flexible, Transparent, and Highly Active SERS. *Anal. Chem.* **2014**, *86*, 6262−7.
(23) Chen, P. X.; Shang, S. B.; Hu, L. T.; Liu, X. Y.; Qiu, H. W.; Li, C. H.; Huo, Y. Y.; Jiang, S. Z.; Yang, C. A suitable for large scale production, flexible and transparent surface-enhanced Raman scattering substrate for in situ ultrasensitive analysis of chemistry reagents. *Chem. Phys. Lett.* **2016**, *660*, 169−175.
(24) Kumar, S.; Goel, P.; Singh, J. P. Flexible and robust SERS active substrates for conformal rapid detection of pesticide residues from fruits. *Sens. Actuators, B* **2017**, *241*, 577−583.
(25) Tian, L.; Jiang, Q.; Liu, K. K.; Luan, J.; Naik, R. R.; Singamaneni, S. Bacterial Nanocellulose-Based Flexible Surface Enhanced Raman Scattering Substrate. *Adv. Mater. Interfaces* **2016**, *3*, 1600214.
(26) Qiu, H.; Wang, M.; Jiang, S.; Zhang, L.; Yang, Z.; Li, L.; Li, J.; Cao, M.; Huang, J. Reliable molecular trace-detection based on flexible SERS substrate of graphene/Ag-nanoflowers/PMMA. *Sens. Actuators, B* **2017**, *249*, 439.
(27) Sun, H.; Liu, H.; Wu, Y. A Flexible and Highly Sensitive Surface−Enhanced Raman Scattering Film in-situ Detection of Malachite Green on Fish Skin. *Mater. Lett.* **2017**, *207*, 125.
(28) Yan, T.; Zhang, L.; Jiang, T.; Bai, Z.; Yu, X.; Dai, P.; Wu, M. Controllable SERS performance for the flexible paper-like films of reduced graphene oxide. *Appl. Surf. Sci.* **2017**, *419*, 373.
(29) Alvarezpuebla, R.; Cui, B.; Bravo-Vasquez, J.-P.; Veres, T.; Fenniri, H. Nanoimprinted SERS-Active Substrates with Tunable Surface Plasmon Resonances. *J. Phys. Chem. C* **2007**, *111*, 6720−6723.
(30) He, D.; Hu, B.; Yao, Q. F.; Wang, K.; Yu, S. H. Large-scale synthesis of flexible free-standing SERS substrates with high sensitivity: electrospun PVA nanofibers embedded with controlled alignment of silver nanoparticles. *ACS Nano* **2009**, *3*, 3993−4002.
(31) Zhang, C. L.; Lv, K. P.; Huang, H. T.; Cong, H. P.; Yu, S. H. Co-assembly of Au nanorods with Ag nanowires within polymer nanofiber matrix for enhanced SERS property by electrospinning. *Nanoscale* **2012**, *4*, 5348−55.
(32) Lee, S. Y.; Kim, S. H.; Kim, M. P.; Jeon, H. C.; Kang, H.; Kim, H. J.; Kim, B. J.; Yang, S. M. Freestanding and Arrayed Nanoporous Microcylinders for Highly Active 3D SERS Substrate. *Chem. Mater.* **2013**, *25*, 2421−2426.
(33) Qian, Y.; Meng, G.; Huang, Q.; Zhu, C.; Huang, Z.; Sun, K.; Chen, B. Flexible membranes of Ag-nanosheet-grafted polyamide-nanofibers as effective 3D SERS substrates. *Nanoscale* **2014**, *6*, 4781.
(34) Zhao, W.; Liu, X.; Xu, Y.; Wang, S.; Sun, T.; Liu, S.; Wu, X.; Xu, Z. Polymer nanopillar array with Au nanoparticle inlays as a flexible and transparent SERS substrate. *RSC Adv.* **2016**, *6*, 35527−35531.
(35) Lee, W. W.; Silverson, V. A.; Jones, L. E.; Ho, Y. C.; Fletcher, N. C.; Mcnaul, M.; Peters, K. L.; Speers, S. J.; Bell, S. E. Surface-enhanced Raman spectroscopy of novel psychoactive substances using polymer-stabilized Ag nanoparticle aggregates. *Chem. Commun.* **2016**, *52*, 493−496.
(36) Lee, W. W.; Mccoy, C. P.; Donnelly, R. F.; Bell, S. E. Swellable polymer films containing Au nanoparticles for point-of-care therapeutic drug monitoring using surface-enhanced Raman spectros-copy. *Anal. Chim. Acta* **2016**, *912*, 111.
(37) Ye, X.; Gao, Y.; Chen, J.; Reifsnyder, D. C.; Zheng, C.; Murray, C. B. Seeded growth of monodisperse gold nanorods using bromide-free surfactant mixtures. *Nano Lett.* **2013**, *13*, 2163−2171.
(38) Karakoti, A. S.; Das, S.; Thevuthasan, S.; Seal, S. PEGylated Inorganic Nanoparticles. *Angew. Chem., Int. Ed.* **2011**, *50*, 1980−1994.
(39) Alkilany, A. M.; Yaseen, A. I. B.; Park, J.; Eller, J. R.; Murphy, C. Facile Phase Transfer of Gold Nanoparticles From Aqueous Solution to Organic Solvents with Thiolated Poly(ethylene glycol). *RSC Adv.* **2014**, *4*, 52676−52679.
(40) Yue, S.; Sun, X.; Wang, N.; Wang, Y.; Wang, Y.; Xu, Z.; Chen, M. L.; Wang, J. H. A SERS-Fluorescence Dual-Mode pH Sensing Method Based on Janus Microparticles. *ACS Appl. Mater. Interfaces* **2017**, *9*, 39699−39707.
(41) Jain, P. K.; Eustis, S.; El-Sayed, M. A. Plasmon coupling in nanorod assemblies: optical absorption, discrete dipole approximation simulation, and exciton-coupling model. *J. Phys. Chem. B* **2006**, *110*, 18243−18253.
(42) Pei, L.; Huang, Y.; Li, C.; Zhang, Y.; Rasco, B. A.; Lai, K. Detection of triphenylmethane drugs in fish muscle by surface-enhanced raman spectroscopy coupled with Au-Ag core-shell nanoparticles. *J. Nanomater.* **2014**, *2014*, 1.
(43) Chen, X.; Nguyen, T. H. D.; Gu, L.; Lin, M. Use of Standing Gold Nanorods for Detection of Malachite Green and Crystal Violet in Fish by SERS. *J. Food Sci.* **2017**, *82*, 1640−1646.
(44) Jia, H. Y.; Zeng, J. B.; Song, W.; An, J.; Zhao, B. Preparation of silver nanoparticles by photo-reduction for surface-enhanced Raman scattering. *Thin Solid Films* **2006**, *496*, 281−287.
(45) K, J.; S, B.; R, D.; Ganiga, M.; George, B. K.; S, A.; Cyriac, J. Effective SERS detection using a flexible wiping substrate based on electrospun polystyrene nanofibers. *Anal. Methods* **2017**, *9*, 3998−4003.
(46) Liao, J.; Wang, D.; Liu, A.; Hu, Y.; Li, G. Controlled stepwise-synthesis of core-shell Au@MIL-100 (Fe) nanoparticles for sensitive surface-enhanced Raman scattering detection. *Analyst* **2015**, *140*, 8165−71.
(47) Song, J.; Huang, Y.; Fan, Y.; Zhao, Z.; Yu, W.; Rasco, B. A.; Lai, K. Detection of Prohibited Fish Drugs Using Silver Nanowires as

DOI: 10.1021/acs.jafc.8b01702
J. Agric. Food Chem. 2018, 66, 6889−6896

Substrate for Surface-Enhanced Raman Scattering. *Nanomaterials* **2016**, *6*, 175.
(48) Xiao, G.; Li, Y.; Shi, W.; Shen, L.; Chen, Q.; Huang, L. Highly sensitive, reproducible and stable SERS substrate based on reduced graphene oxide/silver nanoparticles coated weighing paper. *Appl. Surf. Sci.* **2017**, *404*, 334−341.
(49) Chen, J. M.; Huang, Y. J.; Kannan, P.; Zhang, L.; Lin, Z. Y.; Zhang, J. W.; Chen, T.; Guo, L. H. Flexible and Adhesive Surface Enhance Raman Scattering Active Tape for Rapid Detection of Pesticide Residues in Fruits and Vegetables. *Anal. Chem.* **2016**, *88*, 2149−2155.

DOI: 10.1021/acs.jafc.8b01702
J. Agric. Food Chem. 2018, 66, 6889−6896